

¹⁸F-Florzolotau Positron Emission Tomography Imaging of Tau Pathology in the Living Brains of Patients with Corticobasal Syndrome

Feng-Tao Liu, MD, PhD,¹ Jia-Ying Lu, MD,² Xin-Yi Li, MD,¹ Fang-Yang Jiao, MD,² Ming-Jia Chen, MD,¹ Rui-Xin Yao, MD,¹ Xiao-Niu Liang, PhD,^{1,3} Zi-Zhao Ju, MD,² Jing-Jie Ge, MD, PhD,² Gen Li, MD,¹ Bo Shen, MD,¹ Ping Wu, MD,² Jiong Song, MD,² Ji Li, MD,⁴ Yi-Min Sun, MD, PhD,¹ Jian-Jun Wu, MD, PhD,¹ Tzu-Chen Yen, MD, PhD,⁵ Jian-Feng Luo, MD,⁶ Qian-hua Zhao, MD,¹ Chuantao Zuo, MD, PhD,^{2*} Jian Wang, MD, PhD,^{1*} and for the Progressive Supranuclear Palsy Neuroimage Initiative

¹Department of Neurology, National Research Center for Aging and Medicine, National Center for Neurological Disorders, and State Key Laboratory of Medical Neurobiology, Huashan Hospital, Fudan University, Shanghai, China

²Department of Nuclear Medicine & PET Center, National Center for Neurological Disorders, and National Clinical Research Center for Aging and Medicine, Huashan Hospital, Fudan University, Shanghai, China

³Institute of Neurology, Fudan University, Shanghai, China

⁴Department of Integrated Traditional and Western Medicine, Huashan Hospital, Fudan University, Shanghai, China

⁵APRINOIA Therapeutics Co., Ltd, Suzhou, China

⁶Department of Biostatistics, School of Public Health, Fudan University, Shanghai, China

ABSTRACT: Background: Recent development in tau-sensitive tracers has sparked significant interest in tracking tauopathies using positron emission tomography (PET) biomarkers. However, the ability of ¹⁸F-florzolotau PET imaging to topographically characterize tau pathology in corticobasal syndrome (CBS) remains unclear. Further, the question as to whether disease-level differences exist with other neurodegenerative tauopathies is still unanswered.

Objective: To analyze the topographical patterns of tau pathology in the living brains of patients with CBS using ¹⁸F-florzolotau PET imaging and to examine whether differences with other tauopathies exist.

Methods: ¹⁸F-florzolotau PET imaging was performed in 20 consecutive patients with CBS, 20 cognitively healthy controls (HCs), 20 patients with Alzheimer's disease (AD), and 16 patients with progressive supranuclear palsy–Richardson's syndrome (PSP-RS).

Cerebrospinal fluid (CSF) levels of β -amyloid biomarkers were quantified in all patients with CBS. ¹⁸F-florzolotau uptake was quantitatively assessed using standardized uptake value ratios.

Results: Of the 20 patients with CBS, 19 (95%) were negative for CSF biomarkers of amyloid pathology; of them, three had negative ¹⁸F-florzolotau PET findings. Compared with HCs, patients with CBS showed increased ¹⁸F-florzolotau signals in both cortical and subcortical regions. In addition, patients with CBS were characterized by higher tracer retentions in subcortical regions compared with those with AD and showed a trend toward higher signals in cortical areas compared with PSP-RS. An asymmetric pattern of ¹⁸F-florzolotau uptake was associated with an asymmetry of motor severity in patients with CBS.

Conclusions: In vivo ¹⁸F-florzolotau PET imaging holds promise for distinguishing CBS in the spectrum of

*Correspondence to: Dr. Jian Wang, Department of Neurology, Huashan Hospital, Fudan University, 12 Middle Wulumuqi Road, Shanghai 200040, China, E-mail: wangjian_hs@fudan.edu.cn; Dr. Chuantao Zuo, Department of Nuclear Medicine & PET Center, Huashan Hospital, Fudan University, 518 East Wuzhong Road, Shanghai 200235, China, E-mail: zuochuantao@fudan.edu.cn

F.-T. Liu, J.-Y. Lu, and X.-Y. Li contributed equally to this work.

Relevant conflicts of interest/financial disclosures: Tzu-Chen Yen is an employee of APRINOIA Therapeutics Co., Ltd (Suzhou, China). All other authors declare that they have no conflicts of interest.

Funding agencies: Grants were obtained by J.W. through the Shanghai Municipal Science and Technology Major Project (2018SHZDZX01 and 21S31902200) and the Zhangjiang Lab, the National Health Commission of People's Republic of China (PRC)

(Pro20211231084249000238), and the National Natural Science Foundation of China (82171421, 91949118 and 92249302). F.-T.L. was supported by the National Natural Science Foundation of China (82171252 and 81701250). Grants were obtained by C.Z. through the National Natural Science Foundation of China (82272039, 82021002, 81971641, and 81671239), the Research Project of the Shanghai Health Commission (2020YJZX011), the Clinical Research Plan of Shanghai Hospital Development Center (SHDC) (SHDC2020CR1038B), and the ST12030-Major Project (2022ZD0211600).

Received: 25 October 2022; **Revised:** 28 December 2022; **Accepted:** 17 January 2023

Published online in Wiley Online Library (wileyonlinelibrary.com). DOI: 10.1002/mds.29338

Corticobasal degeneration (CBD) is a rare neurodegenerative tauopathy. The most common clinical presentation of CBD is the corticobasal syndrome (CBS), which is characterized by heterogeneous cortical and basal ganglia disturbances with either unilateral or asymmetric presentation. At present, the diagnosis of CBD can be confirmed only by postmortem pathological examination showing the presence of intracellular fibrillary tangles in which the 4-repeat (4R) isoform of tau predominates.¹ However, apart from CBD, the pathological findings in CBS can be associated with other distinct disorders—including progressive supranuclear palsy (PSP; a primary 4R tauopathy), Alzheimer's disease (AD; a secondary mixed 3R/4R tauopathy), and frontotemporal lobar degeneration with TAR DNA-binding protein 43 (TDP-43) proteinopathy (a nontauopathy).² Therefore, it is difficult to reliably predict neuropathological findings of CBD in patients with CBS.³

In recent years, positron emission tomography (PET) has received growing endorsement for in vivo imaging of tau burden in patients with tauopathies.¹ Although PET imaging for neurofibrillary tau is expected to have a considerable diagnostic value in patients with neurodegenerative diseases,¹ there is still no clinically validated neuroimaging probe to visualize CBD-related tau pathology in the living brain. Notably, previous reports in patients with CBS have expressed concerns that first-generation tau PET tracers may have significant limitations—including low affinity to the 4R isoform of tau,⁴ off-target binding,^{5,6} or limited in vivo stability against metabolic conversion.⁷ Interestingly, a recent study showed increased retentions of the second-generation tau tracer ^{18}F -PI-2620 in the basal ganglia and dorsolateral prefrontal cortex of patients with CBS.⁸ In our previous work,⁹⁻¹¹ we demonstrated that PET imaging with ^{18}F -florzolotau—a second-generation tau radiotracer—may aid in the classification of different tauopathies by highlighting the topographical distribution of tau pathology that underlies the spectrum of disorders. However, the ability of ^{18}F -florzolotau PET imaging to topographically characterize tau deposition in CBS remains unclear. Furthermore, the question as to whether group-level differences exist with other tauopathies is still unanswered. Therefore, in this study we evaluated the patterns of tau pathology in the living brain of patients with CBS using ^{18}F -florzolotau PET imaging and examined whether differences with other tauopathies exist. We also assessed regional uptake as a function of severity and clinical asymmetry.

Methods

Study Participants

All visits and procedures occurred at the Movement Disorders Clinic, Department of Neurology, Huashan Hospital, Fudan University (Shanghai, China). The study started in July 2020 and concluded in July 2022. A total of 20 consecutive patients who met the Movement Disorder Society (MDS)–PSP criteria¹² and the Armstrong criteria¹³ for clinical CBS were enrolled. Patients with a history of traumatic brain injury, stroke, severe depression, or major medical illnesses were excluded, as were individuals who had contraindications to PET imaging and/or magnetic resonance imaging (MRI) (ie, claustrophobia and metal implants) or were unwilling to undergo the study procedures. All clinical features were reviewed by three experienced neurologists (F.-T.L., J.-J.W., and J.W.). Three additional study groups were included for comparison purposes: cognitively healthy controls (HCs; $n = 20$), patients with AD ($n = 20$), and patients with PSP–Richardson's syndrome (PSP-RS; $n = 16$). HCs had no history of neurological or psychiatric disorders; in addition, they did not show any deficit during neurologic examination and had no abnormal findings on brain MRI.⁹ Patients with AD met the 2011 National Institute on Aging and Alzheimer's Association (NIA-AA) diagnostic criteria¹⁴ and had evidence of amyloid pathology on PET imaging. PSP-RS was diagnosed according to the MDS diagnostic criteria.⁹ Both HCs and patients with PSP-RS were included in a prior study focusing on ^{18}F -florzolotau PET imaging.^{9,10} The study protocol was approved by the Ethics Committee of the Huashan Hospital (Fudan University), and all participants or legal guardians provided written informed consent.

Clinical Assessment

All patients with CBS/PSP-RS were assessed after at least 12 hours from the last dose of any anti-parkinsonian medication. Variables collected were age at onset (years), disease duration (months), global cognition (Mini-Mental State Examination [MMSE]), and motor symptoms (MDS Unified Parkinson's Disease Rating Scale [MDS UPDRS] and Progressive Supranuclear Palsy Rating Scale [PSPRs]).⁹ The total levodopa equivalent daily dose was calculated for both patients with CBS and PSP-RS.⁹ MMSE scores were obtained from both HCs and patients with AD. In the latter

group, age at onset (years) and disease duration (months) were also recorded.

Biochemical and Imaging Biomarkers of Amyloid Pathology

Cerebrospinal fluid (CSF) levels of β -amyloid biomarkers ($A\beta_{1-42}$ and $A\beta_{1-40}$) in patients with CBS were quantified using commercial enzyme-linked immunosorbent assays (Euroimmun, Lubeck, Germany) according to the manufacturer's protocol.¹⁵ All assays were performed by certified laboratory technicians at the Oumeng V Medical Laboratory (Hangzhou, China). The thresholds for positivity were based on the laboratory reference ranges. Patients with AD underwent ¹⁸F-Florbetapir amyloid PET imaging. Positivity was defined according to the semiquantitative binary criterion outlined by the Alzheimer's Disease Neuroimaging Initiative (https://adni.bitbucket.io/reference/docs/UCBERKELEYAV45/ADNI_AV45_Methods_JagustLab_06.25.15.pdf).

Image Acquisition and Processing

All imaging procedures were carried out in the Huashan Hospital by experienced nuclear medicine physicians blinded to the clinical data. All ¹⁸F-florzolotau PET scans were acquired within 1 month from clinical assessments according to a previously described methodology.⁹ In brief, participants initially underwent anatomical MRI using a 3.0-T horizontal magnet (Discovery MR750; GE Medical Systems, Milwaukee, WI). Acquisition of static ¹⁸F-florzolotau PET images was performed using a Siemens PET/computed tomography (CT) scanner (micor CT flow PET/CT, Siemens, Erlangen, Germany) 90 to 110 minutes after an intravenous bolus injection of ¹⁸F-florzolotau (370 MBq). All patients with CBS were imaged at baseline, and three of them underwent a second follow-up scan after 1 year. Individual ¹⁸F-florzolotau PET scans were resampled in the common space of the corresponding T1-weighted images and subsequently registered to the Montreal Neurological Institute (MNI) brain template. Spatially normalized PET images were smoothed using a Gaussian kernel (full-width at half-maximum: 6 mm). All procedures were performed using the Statistical Parametric Mapping (SPM) toolbox (version 12; <http://www.fil.ion.ucl.ac.uk/spm/software/spm12/>) implemented in MATLAB (MathWorks, Natick, MA).⁹ The cerebellar gray matter was chosen as the reference for intensity normalization; subsequently, standardized uptake value ratio (SUVR) maps were created for semiquantitative analysis of tracer accumulation.^{9,10} The following 14 cortical regions of interest (ROIs) were selected: bilateral precentral gyrus, postcentral gyrus, supplementary motor area (SMA), frontal cortex, parietal cortex, temporal cortex, and

occipital cortex. We also examined a set of eight subcortical ROIs: bilateral putamen, globus pallidus (GP), subthalamic nucleus (STN), and red nucleus (RN). Cortical ROIs were identified using the automated anatomical atlas three template,¹⁶ whereas the MNI PD25 template was used for subcortical ROIs.¹⁷ On analyzing patients with CBS, region-level comparisons and regional tau PET positivity were based on SUVR values calculated for the hemisphere contralateral to the most affected body side. As for patients with AD, patients with PSP, and HCs, the highest SUVR value extracted from bilateral ROIs was used for the purpose of analysis.

Calculation of SUVR Z Scores and Definition of Tau PET Positivity

We calculated regional SUVR *z* scores using the following formula: $z \text{ score} = (\text{individual patient's SUVR} - \text{mean of bilateral SUVR values observed in HCs}) / \text{standard deviation of the SUVR value observed in HCs}$. In semiquantitative analyses, a regional *z* score ≥ 2 was considered positive.⁹ The presence of at least one positive cortical or subcortical region was the criterion used to define cortical and subcortical positivity, respectively. In accordance with our previous methodology,⁹ global positivity was defined as the presence of at least two positive ROIs on ¹⁸F-florzolotau PET imaging (two-region positivity criterion).

Analysis of Asymmetric ¹⁸F-Florzolotau Uptake

The asymmetric distribution of ¹⁸F-florzolotau uptake was analyzed using a semiquantitative approach in individual regions. The asymmetry index was calculated according to the following formula: $(\text{SUVRs}_{\text{Left}} - \text{SUVRs}_{\text{Right}}) / (\text{SUVRs}_{\text{Left}} + \text{SUVRs}_{\text{Right}}) \times 2 \times 100$. The asymmetry of motor symptoms was calculated using the following index: $(A - B) / (A + B) \times 2 \times 100$,¹⁸ where A and B are the sum of right- and left-sided scores of the MDS UPDRS scale (3.3 to 3.8), respectively.

Statistics

Data normality was checked using the Kolmogorov-Smirnov test. Continuous variables are summarized using means \pm standard deviations or medians and interquartile ranges for non-normally distributed data. Differences between two groups were assessed by Student *t* tests or Mann-Whitney *U* tests as appropriate. One-way analysis of variance or Kruskal-Wallis tests were used to compare normally and non-normally continuous data across four groups, respectively, and post hoc analyses were performed by applying the Bonferroni correction. Proportions were compared using χ^2 tests. A generalized linear model adjusted for age, sex, and disease duration was applied to compare semiquantitative PET data across different target

regions, and the Benjamini–Hochberg procedure was used to adjust the significance threshold for multiple comparisons. The Spearman coefficient of correlation was applied to investigate the associations between the asymmetry index for ^{18}F -florzolotau binding and clinical asymmetry. Partial correlation coefficients adjusted for age and years of education were used to assess the correlations between PET findings and the cognitive function of patients with CBS. Analyses were performed using SPSS, version 22.0 (IBM, Armonk, NY), with all tests two-sided at a 5% level of significance. We used two-sample t tests implemented in SPM to evaluate voxel-level differences in ^{18}F -florzolotau binding across the study groups. When the analysis was carried out in the CBS group, PET images were flipped along the x-axis to merge image data from the hemisphere contralateral to the most affected body side.¹⁹ When deemed appropriate, SUVR images were adjusted for age, sex, and disease duration. Unless otherwise indicated, the cluster-wise threshold for statistical significance was set at a $P < 0.05$ with a false discovery rate correction to safeguard the results for multiple comparisons. This corresponded to an uncorrected voxel-wise P value < 0.001 .

Results

General Characteristics of the Study Participants

The demographic and clinical characteristics of the 20 patients with CBS are presented in Tables 1 and S1. Of them, 19 were negative for CSF biomarkers of amyloid pathology. Compared with patients with tauopathies, HCs were younger and had a better cognitive status. Patients with CBS, AD, and PSP-RS did not differ significantly in terms of age, disease duration, and MMSE scores. However, disease severity, as reflected by MDS UPDRS and PSPrs scores, tended to be higher in patients with CBS than in those with PSP-RS (Table 1).

Distribution of ^{18}F -Florzolotau Binding

Compared with HCs, patients with CBS showed an increased ^{18}F -florzolotau signal in both cortical (ie, precentral gyrus, postcentral gyrus, and SMA) and subcortical (ie, putamen, GP, STN, and RN) regions. (Table 2). An illustrative example of ^{18}F -florzolotau PET findings in a patient with CBS is provided in Figure 1A,B. Cortical retention of ^{18}F -florzolotau was more easily distinguishable in the only case of CBS who tested positive for CSF amyloid biomarkers. In a voxel-wise analysis, an increased ^{18}F -florzolotau uptake was evident in the contralateral precentral gyrus, SMA, and basal ganglia (Fig. 1D and Table S2). When patients with CBS were compared with those with AD, the

former group was characterized by a lower ^{18}F -florzolotau signal in the majority of cortical regions; conversely, higher tracer retention was observed in the contralateral precentral gyrus, SMA, and subcortical regions (ie, GP, STN, and RN; Table 2, Fig. 1E, and Table S3). Compared with patients with PSP-RS, those with CBS showed a trend toward a lower retention in subcortical regions, mainly in the contralateral side (Table 2, Fig. 1F, and Table S4). A comparison between amyloid-negative patients with CBS, AD, and PSP-RS as well as HCs is shown in Table S5.

Tau Positivity in Patients with CBS

Cortical and subcortical regions that met the criteria for tau positivity (threshold >2 standard deviations of values observed in HCs) are reported in Figure 2A. Subcortical regions (ie, GP, STN, and RN) of patients with CBS were more commonly positive than those of patients with AD. Compared with patients with PSP-RS, those with CBS were more frequently characterized by positive cortical regions (especially the precentral gyrus); however, opposite findings were observed for subcortical regions (especially the STN). Detailed data are reported in Table S6.

The previously described two-region positivity criterion⁹ was applied to assign positive versus negative ^{18}F -florzolotau PET findings at the individual level (Fig. 2B). Three (15%) of the 20 patients with CBS had negative results on ^{18}F -florzolotau PET, and all of them tested negative for CSF amyloid biomarkers. On analyzing the regional-level positivity, two patients (10%) were negative in both the cortical and subcortical regions (C-S-), three (15%) were positive in the cortical and negative in subcortical regions (C + S-), and 15 (75%) were positive in both the cortical and subcortical regions (C + S+). Figure 2B shows the individual distribution of positive findings based on ^{18}F -florzolotau PET imaging data and CSF amyloid biomarkers.

Associations Between ^{18}F -Florzolotau Uptake and Clinical Symptoms

As indicated in Figure 3A–C, the asymmetric index of ^{18}F -florzolotau uptake in the precentral gyrus ($r = 0.466$, $P = 0.039$), putamen ($r = 0.687$, $P = 0.001$), and GP ($r = 0.753$, $P < 0.001$) of patients with CBS was positively associated with the motor asymmetric index calculated from MDS UPDRS scores. After adjustment for age and years of education in partial correlation analyses (uncorrected for multiple comparisons), SUVR values in the occipital cortex ($r = -0.488$, $P = 0.047$) and temporal cortex ($r = -0.543$, $P = 0.024$) were inversely correlated with MMSE scores. No association between MDS UPDRS

TABLE 1 General characteristics of the four study groups

	CBS	AD	PSP-RS	HCs	P	Post hoc P
Number of subjects	20	20	16	20	—	—
Sex, men/women	7/13	7/13	9/7	6/14	0.408	—
Age, years	68.80 ± 8.90	65.60 ± 8.78	64.00 ± 7.26	56.65 ± 7.29	<0.001	<0.001, ^a 0.005 ^b
Education, years	9.00 (8.25, 14.25)	9.00 (6.00, 10.75)	11.00 (8.00, 14.75)	12.00 (9.00, 15.75)	0.110	—
Disease duration, months	32.00 (23.25, 46.50)	24.00 (12.00, 36.00)	36.50 (22.75–51.00)	—	0.081	—
MMSE	21.00 (17.00, 26.00)	20.00 (19.00, 22.00)	25.00 (19.50, 26.75)	28.00 (27.00, 29.00)	<0.001	<0.001, ^a <0.001, ^b 0.003 ^c
MDS UPDRS-III	47.65 ± 20.05	—	36.13 ± 15.18	—	0.066	—
PSPrs	41.00 (27.75, 53.25)	—	26.00 (19.75, 34.75)	—	0.032	—
LEDD	350.00 (0.00, 584.38)	—	600.00 (400.00–750.00)	—	0.099	—

Note: Data are expressed as n, mean ± standard deviation, or median (interquartile range), as appropriate. Post hoc P values were calculated after applying the Bonferroni correction. Abbreviations: CBS, corticobasal syndrome; AD, Alzheimer’s disease; PSP-RS, progressive supranuclear palsy–Richardson’s syndrome; HCs, healthy controls; MMSE, Mini-Mental State Examination; MDS UPDRS, Movement Disorders Society Unified Parkinson’s Disease Rating Scale; PSPrs, Progressive Supranuclear Palsy Rating Scale; LEDD, levodopa equivalent daily dose.
^aPatients with CBS vs. HCs.
^bPatients with AD vs. HCs.
^cPatients with PSP-RS vs. HCs.

and PSPrs scores and ¹⁸F-florzolotau SUVR values was observed.

Longitudinal Analysis

Three of the 20 patients with CBS underwent a follow-up ¹⁸F-florzolotau PET scan 1 year after the baseline assessment (Table S7). Two of them had positive ¹⁸F-florzolotau PET findings at baseline, whereas the remaining case had negative results. In the former group, one patient showed an increased tracer uptake at follow-up (Fig. 3D), whereas the other did not (Fig. 3E). However, MDS UPDRS and PSPrs scores did not change appreciably over time in both patients (Table S7). As for the case with negative ¹⁸F-florzolotau PET findings at baseline, disease severity increased at follow-up (Table S7), but imaging data remained negative (Fig. 3F).

Discussion

In this study, we used ¹⁸F-florzolotau PET imaging to analyze the topographical distribution of tau accumulation in the living brain of patients with CBS. We also compared the observed signals with those found in other tauopathies and correlated the patterns of ¹⁸F-florzolotau uptake with disease severity and clinical asymmetry. We emphasize three major findings. First, patients with CBS showed an increased ¹⁸F-

florzolotau signal in both cortical (ie, precentral gyrus, postcentral gyrus, and SMA) and subcortical (ie, GP, STN, and RN) regions compared with HCs. This was seen in patients with either negative or positive amyloid status. Second, the distribution and intensity of ¹⁸F-florzolotau signal in CBS were found to differ from those observed in both AD and PSP-RS. Pending independent confirmation in larger cohorts, these findings show potential for ¹⁸F-florzolotau PET as an imaging biomarker for differential diagnosis in patients with tauopathies. Finally, an asymmetric pattern of ¹⁸F-florzolotau retention in the precentral gyrus, putamen, and GP was associated with an asymmetry of motor severity.

When interpreting tau PET imaging findings in CBS, it is paramount to disentangle the effects of concomitant amyloid pathology. A meta-analysis of post-mortem studies showed the presence of AD pathology in 18% of cases who were clinically diagnosed with CBS.²⁰ In addition, prior PET investigations focusing on CBS identified AD pathology in 0% to 47% of cases.^{21–23} This has some contrasts to our study, where only one of the 20 patients with CBS (5%) was amyloid positive; this can be explained by the small sample size and/or a bias related to recruitment from a movement disorders clinic. We therefore reasoned that the underlying pathology in the remaining 19 patients was either 4R tauopathy or unrelated to tau deposition.

TABLE 2 SUVRs of ¹⁸F-florzolotau binding for different brain regions in the four study groups

Brain region	CBS	AD	PSP-RS	HCs	P* CBS vs. AD	P** CBS vs. PSP-RS	P*** CBS vs. HCs
Cortical regions							
Precentral gyrus	1.13 ± 0.25	1.23 ± 0.20	0.98 ± 0.14	0.92 ± 0.07	0.596	0.210	0.003 ^a
Postcentral gyrus	1.03 ± 0.17	1.23 ± 0.22	0.94 ± 0.14	0.90 ± 0.06	0.022 ^b	0.365	0.010 ^a
Supplementary motor area	1.12 ± 0.22	1.33 ± 0.30	1.01 ± 0.14	0.92 ± 0.09	0.148	0.606	0.020 ^a
Frontal cortex	1.02 ± 0.17	1.41 ± 0.34	0.97 ± 0.14	0.91 ± 0.06	<0.001 ^b	0.909	0.051
Parietal cortex	1.07 ± 0.21	1.52 ± 0.30	1.00 ± 0.15	0.94 ± 0.05	<0.001 ^b	0.805	0.096
Temporal cortex	1.13 ± 0.25	1.67 ± 0.35	1.09 ± 0.17	1.01 ± 0.06	<0.001 ^b	0.917	0.318
Occipital cortex	1.16 ± 0.28	1.60 ± 0.32	1.11 ± 0.12	1.05 ± 0.06	<0.001 ^b	0.917	0.365
Subcortical regions							
Putamen	1.40 ± 0.18	1.42 ± 0.23	1.37 ± 0.21	1.15 ± 0.12	0.824	0.805	<0.001 ^a
Globus pallidus	1.58 ± 0.23	1.34 ± 0.20	1.72 ± 0.25	1.27 ± 0.12	0.009 ^b	0.292	<0.001 ^a
Subthalamic nucleus	1.66 ± 0.36	1.27 ± 0.20	2.00 ± 0.38	1.37 ± 0.13	0.002 ^b	0.124	0.004 ^a
Red nucleus	1.64 ± 0.32	1.33 ± 0.23	1.96 ± 0.37	1.36 ± 0.09	0.005 ^b	0.179	<0.001 ^a

Note: Data are expressed as mean ± standard deviation. When the analysis was carried out in the CBS group, positron emission tomography images were flipped along the x-axis to merge image data from the hemisphere contralateral to the most affected body side, and the SUVR values from the contralateral side were used for the purpose of region-level comparisons. As for patients with AD, patients with PSP, and HCs, the highest SUVR values extracted from bilateral regions of interests were used for the purpose of region-level comparisons. The Benjamini-Hochberg procedure was used to adjust the significance threshold for multiple comparisons.

Abbreviations: SUVR, standardized uptake value ratio; CBS, corticobasal syndrome; AD, Alzheimer's disease; PSP-RS, progressive supranuclear palsy-Richardson's syndrome; HCs, healthy controls.

*Patients with CBS vs. patients with AD.

**Patients with CBS vs. patients with PSP-RS.

***Patients with CBS vs. HCs.

^aStatistically significant difference after applying the post hoc correction for multiple comparisons and adjustment for age and sex.

^bStatistically significant difference after applying the post hoc correction for multiple comparisons and adjustment for age, sex, and disease duration.

The increased ¹⁸F-florzolotau signal seen in the cortical regions (precentral gyrus, postcentral gyrus, and SMA) of our patients with CBS is consistent with the cortical patterns of neurofibrillary tangle distribution in CBD.²⁴ These observations further support the ability of ¹⁸F-florzolotau to track 4R tau pathology^{20,25} and are concordant with previous imaging findings obtained in patients with PSP⁹ or harboring *MAPT* mutations,¹¹ two conditions in which the 4R form of tau predominates. In addition, a previous comparison of tau PET tracers showed that ¹⁸F-florzolotau outperforms ¹⁸F-AV-1451 in terms of affinity for 4R tau.²⁶ Importantly, for patients with CBS who were found to be ¹⁸F-florzolotau negative in our study (3/20; 15%), a nontau neuropathology can be anticipated, which would be in line with previous postmortem findings.²⁰

In concordance with earlier data obtained with another tau tracer (¹⁸F-PI-2620),⁸ cortical ¹⁸F-florzolotau signals in the patient with CBS who showed an abnormal amyloid status were more diffuse and intense than those observed in amyloid-negative CBS. Although the possibility that ¹⁸F-florzolotau can cross-react with amyloid deposits does not appear entirely

warranted according to in vivo and in vitro data obtained in AD,⁷ future longitudinal and postmortem studies should examine this hypothesis more rigorously. Regardless of their amyloid status, patients with CBS showed an increased ¹⁸F-florzolotau uptake in the pre- and postcentral gyrus—two areas that are generally free from tau deposits in amnesic AD.^{8,27} Longitudinal and clinicopathological validation studies are needed to evaluate the hypothesis that an elevated ¹⁸F-florzolotau signal in these cortical areas may serve as a biomarker of CBS.

The ¹⁸F-florzolotau PET findings presented herein also support an increased tracer uptake in subcortical regions of patients with CBS—a pattern with similarities to PSP.⁹ On analyzing ¹⁸F-PI-2620 signals in patients with CBS and PSP-RS, Palleis and colleagues⁸ reported distinct findings for the two conditions—with the former being characterized by an increased tracer uptake in the putamen and external GP and the latter in the internal GP, STN, and substantia nigra. However, our observations did not show obvious differences in terms of positivity or negativity ratios but were limited to quantitative analysis. In light of similar results concerning glucose metabolism²⁸ as

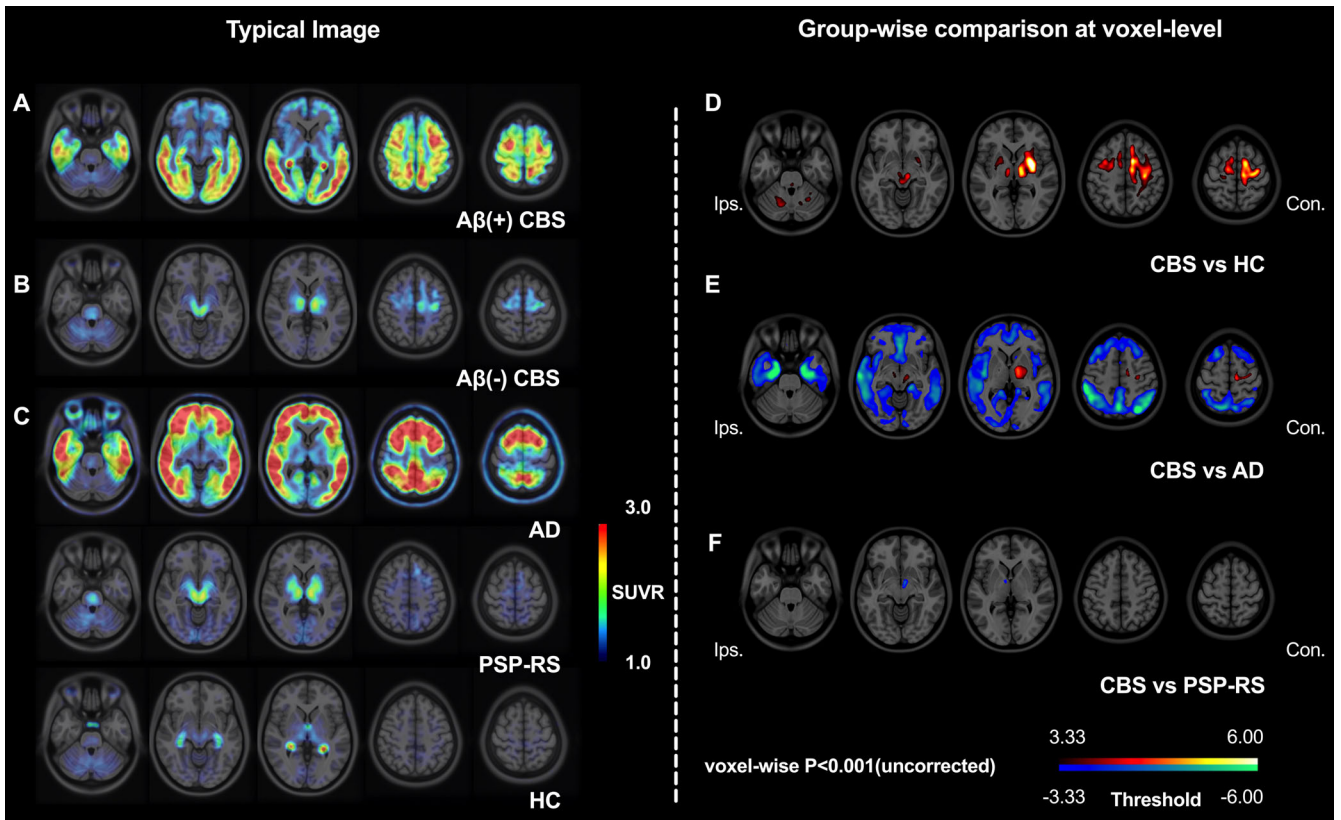


FIG. 1. ¹⁸F-florzolotau binding patterns in patients with corticobasal syndrome (CBS); Alzheimer’s disease (AD); progressive supranuclear palsy–Richardson’s syndrome (PSP-RS); and a cognitively healthy control (HC). Individual and group-wise comparison images are shown on the left and right sides of the vertical dashed line, respectively. Illustrative findings from (A) a 64-year-old female patient with amyloid-positive CBS (disease duration, 8 months); (B) a 63-year-old female patient with amyloid-negative CBS (disease duration, 54 months); and (C) a 66-year-old female patient with AD (upper panel; disease duration, 12 months), a 60-year-old female patient with PSP-RS (middle panel; disease duration, 60 months), and a 63-year-old female cognitively HC (lower panel). Group-wise comparisons of ¹⁸F-florzolotau binding patterns (D) compared with cognitively HCs, patients with CBS showed higher signals in the precentral gyrus, supplementary motor area, and basal ganglia—mainly in the contralateral side ($P < 0.001$); (E) compared with patients with AD, those with CBS showed lower signals in the majority of cortical regions, the only exceptions being the contralateral precentral gyrus and the supplementary motor area (these regions—along with contralateral subcortical areas [ie, globus pallidus, subthalamic nucleus, and red nucleus]—were characterized by higher signals in CBS than AD; $P < 0.001$); and (F) compared with patients with PSP-RS, those with CBS showed slightly lower signals in the midbrain ($P < 0.001$). Con., contralateral; Ips., ipsilateral; SUVR, standardized uptake value ratio. [Color figure can be viewed at wileyonlinelibrary.com]

well as partially overlapping clinical phenotypes,²⁹ further studies are necessary to more precisely determine the groupwise discrimination performance of ¹⁸F-florzolotau PET imaging between CBS and PSP. It is also worth noting that 15% of our patients with CBS were tau positive in cortical regions but tau negative in subcortical areas. These data indicate that tau pathology initially occurs in forebrain structures. In this regard, there is evidence that the propagation of neuronal and glial tau pathology in CBD starts from the frontoparietal and motor cortical areas as well as the striatum, further extends to additional subcortical nuclei, and finally affects the brainstem.³⁰⁻³²

Toward the eventual goal of analyzing ¹⁸F-florzolotau uptake as a function of severity and clinical asymmetry, our current data also provide evidence for an association between an asymmetric pattern of binding and an asymmetry of motor severity, a notion

supported by prior PET studies conducted with other probes.^{8,33}

Albeit limited to three patients who were followed-up for 1 year, we did not find evidence for the ability of ¹⁸F-florzolotau PET imaging to predict the longitudinal trajectories of CBS over time. This was expected in light of the anecdotal nature of this exploratory analysis and the heterogeneous nature of CBS. In addition, negative tau pathology in CBS may be found in the event of rare neuro-pathological alterations, including synucleinopathies, TDP-43 proteinopathies, fused in sarcoma proteinopathy, prion disease (Creutzfeldt–Jakob disease), and cerebrovascular disease.¹ Further longitudinal investigations in a larger sample can assist in our understanding of how best to harness the prognostic potential of ¹⁸F-florzolotau PET imaging.

One of the strengths of our study was the inclusion of patients with AD and PSP-RS, enabling exploration of diagnosis-specific differences in terms of distribution

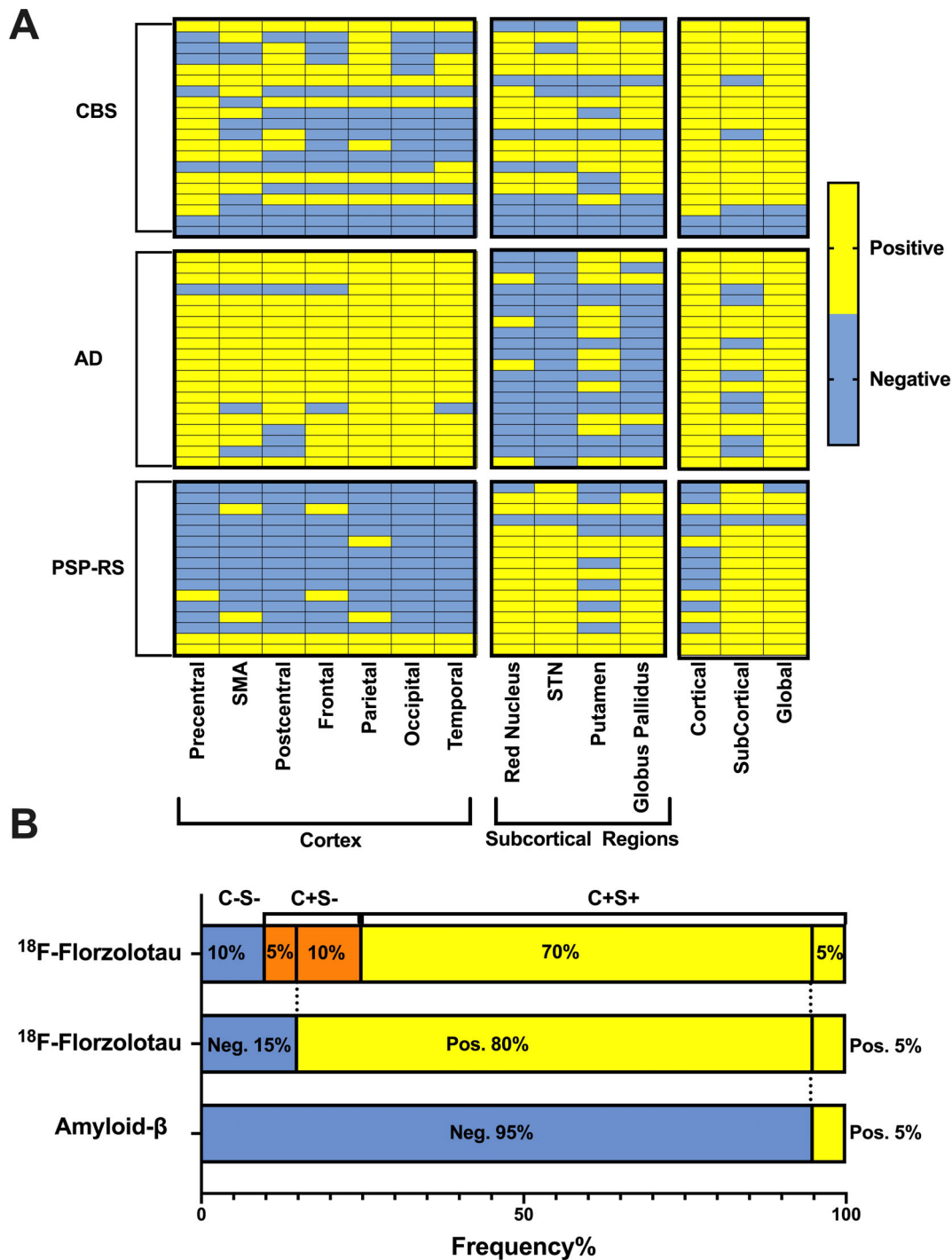


FIG. 2. Differences in regional ¹⁸F-florzolotau uptake in patients with corticobasal syndrome (CBS), Alzheimer’s disease (AD), and progressive supranuclear palsy–Richardson’s syndrome (PSP-RS). **(A)** Distribution of positive (yellow color) and negative (gray color) findings observed in different cortical (C) and subcortical (S) regions of patients with CBS, AD, and PSP-RS. **(B)** Individual distribution of positive findings based on ¹⁸F-florzolotau PET imaging data and cerebrospinal fluid amyloid biomarkers. A summary of region-level positivity (upper panel), individual-level positivity (middle panel), and amyloid status (lower panel) is shown. Neg., negative; Pos., positive; SMA, supplementary motor area; STN, subthalamic nucleus. [Color figure can be viewed at wileyonlinelibrary.com]

and intensity of ¹⁸F-florzolotau signals across tauopathies. Furthermore, this is the first study to explore the value of ¹⁸F-florzolotau PET imaging in patients with CBS. However, our findings need to be interpreted

in the context of several limitations. First, the sample size may not have been sufficiently large to identify other significant differences across diagnostic groups and, for that reason, replication in larger independent samples

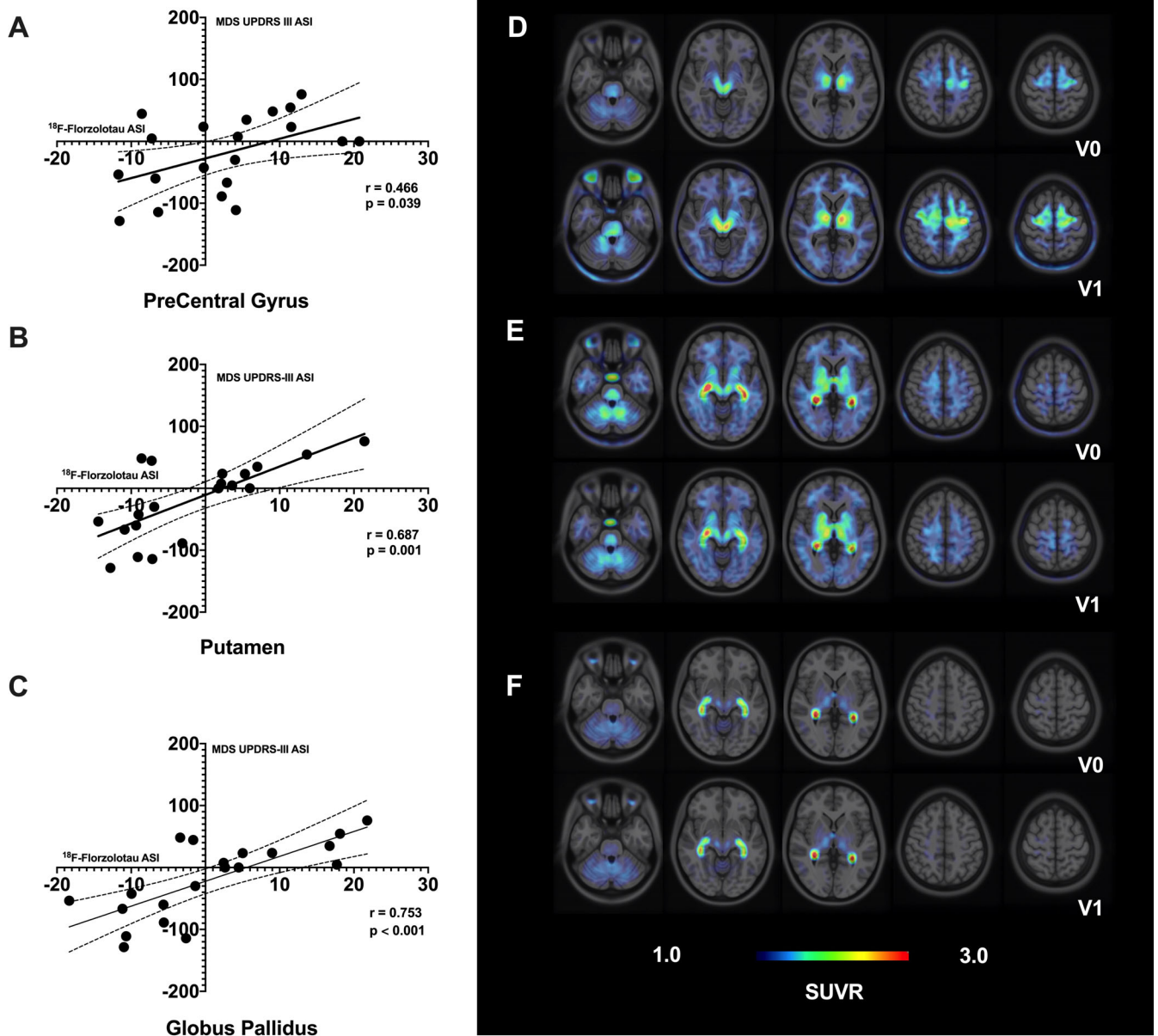


FIG. 3. Associations between ¹⁸F-florzolotau uptake and clinical symptoms. The asymmetric index of ¹⁸F-florzolotau uptake in the (A) precentral gyrus ($r = 0.466$, $P = 0.039$), (B) putamen ($r = 0.687$, $P = 0.001$), and (C) globus pallidus ($r = 0.753$, $P < 0.001$) of patients with corticobasal syndrome (CBS) was positively associated with the motor asymmetric index calculated from Movement Disorders Society Unified Parkinson's Disease Rating Scale (MDS UPDRS) scores. Three patients with CBS underwent a follow-up ¹⁸F-florzolotau positron emission tomography (PET) scan 1 year after baseline assessment. (D) Increased tracer uptake at follow-up in a 64-year-old female patient with positive ¹⁸F-florzolotau PET findings at baseline. (E) The tracer uptake at follow-up did not increase significantly compared with baseline values in a 59-year-old female patient with positive ¹⁸F-florzolotau PET findings. (F) No tracer uptake observed at follow-up in a 70-year-old female patient with negative ¹⁸F-florzolotau PET findings at baseline. ASI, asymmetrical index; SUVR, standardized uptake value ratio; V0, the visit at baseline; V1, the visit at follow-up. [Color figure can be viewed at wileyonlinelibrary.com]

is paramount to confirm and expand our data. Second, it would have been interesting to include a higher number of patients with CBS characterized by an abnormal amyloid status; a larger sample size might have improved the power of the study to analyze its potential confounding effect. Third, we had no data concerning imaging and/or biochemical markers of amyloid pathology in cognitively HCs; we also admit that only one patient with CBS who had a positive CSF amyloid status was subjected to

amyloid PET imaging. Lastly, the clinical nature of the diagnostic process implemented in our study could be prone to misclassifications; however, as mentioned previously, our goal was to investigate an imaging biomarker of tau pathology in the living brain.

There are as yet no imaging biomarkers to distinguish CBS in the spectrum of neurodegenerative tauopathies. Our findings suggest that in vivo ¹⁸F-florzolotau PET imaging holds promise in the differential diagnosis of

CBS. Its clinical significance, however, remains to be explored, and longitudinal data and clinicopathological verification will be needed to further understand its importance. ■

Acknowledgments: We wish to express our gratitude to all of the study participants and their relatives. We thank APRINOIA Therapeutics for the provision of the ^{18}F -florzolotau precursor. We are grateful to Xi-Xi Han, Yi Chen, Ying-Jun Hu, and Jia Zhang (PAWEI Health Promotion Center for Parkinsonism, Shanghai, China) for volunteering in the study.

Data Availability Statement

The datasets generated during and/or analyzed during the current study are available from the corresponding author on reasonable request.

References

- Koga S, Josephs KA, Aiba I, Yoshida M, Dickson DW. Neuropathology and emerging biomarkers in corticobasal syndrome. *J Neurol Neurosurg Psychiatry* 2022;93(9):919–929.
- Ling H, O'Sullivan SS, Holton JL, et al. Does corticobasal degeneration exist? A clinicopathological re-evaluation. *Brain* 2010;133(Pt 7):2045–2057.
- Shelley BP, Hodges JR, Kipps CM, Xuereb JH, Bak TH. Is the pathology of corticobasal syndrome predictable in life? *Mov Disord* 2009;24(11):1593–1599.
- Josephs KA, Whitwell JL, Tacik P, et al. [18F]AV-1451 tau-PET uptake does correlate with quantitatively measured 4R-tau burden in autopsy-confirmed corticobasal degeneration. *Acta Neuropathol* 2016;132(6):931–933.
- Perez-Soriano A, Arena JE, Dinelle K, et al. PBB3 imaging in parkinsonian disorders: evidence for binding to tau and other proteins. *Mov Disord* 2017;32(7):1016–1024.
- Ishiki A, Harada R, Kai H, et al. Neuroimaging-pathological correlations of [^{18}F] THK5351 PET in progressive supranuclear palsy. *Acta Neuropathol Commun* 2018;6(1):53.
- Tagai K, Ono M, Kubota M, et al. High-contrast In vivo imaging of tau pathologies in Alzheimer's and non-Alzheimer's disease tauopathies. *Neuron* 2021;109(1):42–58.e8.
- Palleis C, Brendel M, Finze A, et al. Cortical [^{18}F]PI-2620 binding differentiates corticobasal syndrome subtypes. *Mov Disord* 2021;36(9):2104–2115.
- Li L, Liu FT, Li M, et al. Clinical utility of ^{18}F -APN-1607 tau PET imaging in patients with progressive supranuclear palsy. *Mov Disord* 2021;36(10):2314–2323.
- Liu FT, Li XY, Lu JY, et al. ^{18}F -Florzolotau tau positron emission tomography imaging in patients with multiple system atrophy-parkinsonian subtype. *Mov Disord* 2022;37(9):1915–1923.
- Zhou XY, Lu JY, Liu FT, et al. In vivo ^{18}F -APN-1607 tau positron emission tomography imaging in MAPT mutations: cross-sectional and longitudinal findings. *Mov Disord* 2022;37(3):525–534.
- Höglinger GU, Respondek G, Stamelou M, et al. Clinical diagnosis of progressive supranuclear palsy: the movement disorder society criteria. *Mov Disord* 2017;32(6):853–864.
- Armstrong MJ, Litvan I, Lang AE, et al. Criteria for the diagnosis of corticobasal degeneration. *Neurology* 2013;80(5):496–503.
- McKhann GM, Knopman DS, Chertkow H, et al. The diagnosis of dementia due to Alzheimer's disease: recommendations from the National Institute on Aging-Alzheimer's Association workgroups on diagnostic guidelines for Alzheimer's disease. *Alzheimer's Dement* 2011;7(3):263–269.
- Palmqvist S, Zetterberg H, Mattsson N, et al. Detailed comparison of amyloid PET and CSF biomarkers for identifying early Alzheimer disease. *Neurology* 2015;85(14):1240–1249.
- Rolls ET, Huang CC, Lin CP, Feng J, Joliot M. Automated anatomical labelling atlas 3. *Neuroimage* 2020;206:116189.
- Xiao Y, Fonov V, Chakravarty MM, et al. A dataset of multi-contrast population-averaged brain MRI atlases of a Parkinson's disease cohort. *Data Brief* 2017;12:370–379.
- Liu SY, Wu JJ, Zhao J, et al. Onset-related subtypes of Parkinson's disease differ in the patterns of striatal dopaminergic dysfunction: a positron emission tomography study. *Parkinsonism Relat Disord* 2015;21(12):1448–1453.
- Liu FT, Lu JY, Sun YM, et al. Dopaminergic dysfunction and glucose metabolism characteristics in Parkin-induced early-onset Parkinson's disease compared to genetically undetermined early-onset Parkinson's disease. *Phenomics* 2022.
- Parmera JB, Rodriguez RD, Studart Neto A, Nitrini R, Brucki SMD. Corticobasal syndrome: A diagnostic conundrum. *Dement Neuropsychol* 2016;10(4):267–275.
- Nicolini F, Wilson H, Hirschbichler S, et al. Disease-related patterns of in vivo pathology in corticobasal syndrome. *Eur J Nucl Med Mol Imaging* 2018;45(13):2413–2425.
- Benvenuto A, Guedj E, Felician O, et al. Clinical phenotypes in corticobasal syndrome with or without amyloidosis biomarkers. *J Alzheimers Dis* 2020;74(1):331–343.
- Parmera JB, Coutinho AM, Aranha MR, et al. FDG-PET patterns predict amyloid deposition and clinical profile in corticobasal syndrome. *Mov Disord* 2021;36(3):651–661.
- Beyer L, Meyer-Wilmes J, Schönecker S, et al. Clinical routine FDG-PET imaging of suspected progressive supranuclear palsy and corticobasal degeneration: a gatekeeper for subsequent tau-PET imaging? *Front Neurol* 2018;9:483.
- Endo H, Shimada H, Sahara N, et al. In vivo binding of a tau imaging probe, [^{11}C] PBB3, in patients with progressive supranuclear palsy. *Mov Disord* 2019;34(5):744–754.
- Su Y, Fu J, Yu J, et al. Tau PET imaging with [18F]PMP-PBB3 in frontotemporal dementia with MAPT mutation. *J Alzheimer's Dis* 2020;76(1):149–157.
- Brendel M, Barthel H, van Eimeren T, et al. Assessment of 18F-PI-2620 as a biomarker in progressive supranuclear palsy. *JAMA Neurol* 2020;77(11):1408–1419.
- Niethammer M, Tang CC, Feigin A, et al. A disease-specific metabolic brain network associated with corticobasal degeneration. *Brain* 2014;137(Pt 11):3036–3046.
- Höglinger GU. Is it useful to classify progressive supranuclear palsy and Corticobasal degeneration as different disorders? *Mov Disord Clin Pract* 2018;5(2):141–144.
- Dickson DW. Neuropathologic differentiation of progressive supranuclear palsy and corticobasal degeneration. *J Neurol* 1999;246(Suppl 2):II6–II15.
- Kouri N, Whitwell JL, Josephs KA, Rademakers R, Dickson DW. Corticobasal degeneration: a pathologically distinct 4R tauopathy. *Nat Rev Neurol* 2011;7(5):263–272.
- Kovacs GG, Xie SX, Robinson JL, et al. Sequential stages and distribution patterns of aging-related tau astroglialopathy (ARTAG) in the human brain. *Acta Neuropathol Commun* 2018;6(1):50.
- Kikuchi A, Okamura N, Hasegawa T, et al. In vivo visualization of tau deposits in corticobasal syndrome by ^{18}F -THK5351 PET. *Neurology* 2016;87(22):2309–2316.

Supporting Data

Additional Supporting Information may be found in the online version of this article at the publisher's web-site.

SGML and CITI Use Only
DO NOT PRINT

Author Roles

(1) Research Project: A. Conception, B. Organization, C. Execution; (2) Statistical Analysis: A. Design, B. Execution, C. Review and Critique; (3) Manuscript: A. Writing of the First Draft, B. Review and Critique.

F.-T.L.: 1A, 1B, 1C, 2A, 2B, 2C, 3A, 3B

J.-Y.L.: 1A, 1B, 1C, 2A, 2B, 2C, 3A, 3B

X.-Y.L.: 1A, 1B, 1C, 2A, 2B, 2C, 3A, 3B

F.-Y.J.: 1A, 1B, 1C, 2A, 2C, 3B

M.-J.C.: 1A, 1B, 1C, 2A, 2C, 3B

R.-X.Y.: 1A, 1B, 1C, 2A, 2C, 3B

X.-N.L.: 1A, 1B, 1C, 2A, 2C, 3B

Z.-Z.J.: 1A, 1B, 1C, 2A, 2C, 3B

J.-J.G.: 1A, 1B, 1C, 2A, 2C, 3B

G.L.: 1A, 1B, 1C, 2A, 2C, 3B

B.S.: 1A, 1B, 1C, 2A, 2C, 3B

P.W.: 1A, 1B, 1C, 2A, 2C, 3B

J.S.: 1A, 1B, 1C, 2A, 2C, 3B

J.L.: 1A, 1B, 1C, 2A, 2C, 3B

Y.-M.S.: 1A, 1B, 1C, 2C, 3B

J.-J.W.: 1A, 1B, 1C, 2C, 3B

T.-C.Y.: 1A, 1B, 1C, 2C, 3B

J.-F.L.: 1A, 1B, 1C, 2C, 3B

Q.-H.Z.: 1A, 1B, 1C, 2C, 3B

C.Z.: 1A, 1B, 1C, 2C, 3B

J.W.: 1A, 1B, 1C, 2C, 3B

Full financial disclosures for the previous 12 months

Tzu-Chen Yen is an employee of APRINOIA Therapeutics Co., Ltd (Suzhou, China). All other authors declare that they have no conflicts of interest.